

Abstract objective function graphs on the 3-cube

a classification by realizability

Report

Author(s):

Gärtner, Bernd; Kaibel, Volker

Publication date:

1998

Permanent link:

<https://doi.org/10.3929/ethz-a-006652780>

Rights / license:

[In Copyright - Non-Commercial Use Permitted](#)

Originally published in:

Technical report / Departement of Computer Science, ETH Zürich 296

Abstract Objective Function Graphs on the 3-cube – A Classification by Realizability

Bernd Gärtner* Volker Kaibel†

Abstract

We call an orientation of the graph of a simple polytope P an *abstract objective function (AOF) graph* if it satisfies two conditions that make the simplex algorithm (e.g. with the RANDOM-FACET pivot rule of Kalai [8] and Matoušek, Sharir, and Welzl [10]) work: it has to be acyclic and it has to induce a unique sink in every subgraph that corresponds to a face of the polytope. For the graph of the 3-dimensional cube we investigate the question which among all possible AOF graphs are *realizable* in the sense that they are induced by some linear program (with a polytope of feasible solutions that is combinatorially a 3-dimensional cube). It turns out that (up to isomorphism) precisely two AOF graphs are not realizable.

1 Introduction

Many combinatorial generalizations of linear programming (LP) have been developed and studied in the past, mostly in connection with the simplex algorithm (see [3] for an excellent introduction to LP and the simplex method). Among them are *abstract polytopes* [1], *completely unimodal numberings* [12], *LP-type problems* [10], *abstract optimization problems* [4], and *abstract objective functions* [9]. Such “abstractions” on the one hand allow to argue on a completely combinatorial level, without having to worry about concrete coordinates. On the other hand, they are able to isolate exactly the properties of LP that are needed in a specific context. In many cases, arguments become simpler (see [9] for a striking example) and results more general (here, [10] is not less striking). A well-studied application of generalized LP frameworks is the analysis of randomized simplex variants for linear and more general optimization problems [4, 6, 9, 10, 12].

In this paper we introduce the notion of *AOF graphs*, a concept closely related to Kalai’s *abstract objective functions* (AOF). An AOF orders the vertices of a simple polytope P by ‘height’ in such a way that every face F of P has a *unique* vertex v of smaller height than all its neighbors in the face F . Equivalently, v is at the same time a local and a global height minimum within the face F , a property that allows to check for optimality by considering only the local situation. In fact, the possibility of such a local optimality check is the foundation of the simplex method, and it is also the basis of all the abstract frameworks mentioned above.

An AOF induces an orientation of $G(P)$ – the graph of vertices and edges of P – in a natural way: a directed edge (v, w) exists between adjacent vertices if and only if v has larger height than w . In considering AOF graphs, we identify AOFs which lead to the same edge orientation

*Institut für Theoretische Informatik, ETH Zürich, ETH-Zentrum, CH-8092 Zürich, Switzerland (gaertner@inf.ethz.ch)

†Institut für Informatik, Universität zu Köln, Pohligstr. 1, D-50969 Köln, Germany (kaibel@informatik.uni-koeln.de)

in $G(P)$. This is motivated by the fact that the behavior of many pivot rules for the simplex algorithm only depends on the edge orientations in the polytope graph induced by the objective function. Well-known rules of this type are Bland's rule [2], Zadeh's *Least Entered* rule [13], and many randomized rules, see e.g. [6].

As already indicated, results that are obtained within abstract frameworks can in many cases directly be applied to LP. For example, an upper bound on the runtime of a simplex variant for generalized linear programming problems is also a bound for linear programming itself [10]. On the other hand, consider a generalized linear program on which a certain simplex variant is provably *slow* (such examples have been constructed for RANDOM-FACET by Matoušek [11]); then we have *a priori* no clue whether a linear program with a similar property exists. In this case, one needs to attack the *realizability question*: is a particular instance of an abstract class also an instance of linear programming, or more general: can one identify the linear programming instances among the abstract examples?

In this paper, we solve the realizability question for all AOF graphs on the 3-cube; although this is a problem of constant size only, its solution is quite unexpected and has already led to further insights concerning the realizability question related with Matoušek's above mentioned slow examples for RANDOM-FACET [5].

The rest of the paper is organized as follows: in Section 2 we classify the AOF graphs on the 3-cube according to a simple criterion, in order to reduce the number of cases to be considered later. Realizations for the realizable AOF graphs on the 3-cube are given in Section 3. Finally, in Section 4 the only two (up to isomorphism) non-realizable AOF graphs on the 3-cube are exhibited.

Before we get started, let us make the notions that we will use more precise. Let $G(P) = (V(P), E(P))$ be the graph of vertices and edges of a simple polytope P . A map $\psi : E(P) \rightarrow V(P) \times V(P)$ with $\psi(\{v, w\}) \in \{(v, w), (w, v)\}$ is called an *orientation* of $G(P)$. The directed graph arising from the orientation ψ of $G(P)$ is denoted by $G_\psi(P)$. We usually write $v \rightarrow w$ if $\psi(\{v, w\}) = (v, w)$ and $w \rightarrow v$ otherwise. $G_\psi(P)$ is called an *AOF graph* on P if it is acyclic and for every non-empty face F of P , the subgraph $G_\psi(F)$ induced by the vertices of F has precisely one sink. Note that this does not necessarily imply that every non-empty face has also a unique source. However, in case of the (combinatorial) d -cube C^d this is true (for edges and 2-faces it is obvious, and for $k \geq 3$, it is not hard to see that two sources in a k -face imply a directed cycle if there is no $(k - 1)$ -face with two sources).

An AOF graph $G_\psi(P)$ on P is called *realizable* if there is some polytope $P' \subset \mathbb{R}^d$ (combinatorially equivalent to P) and a linear functional $\phi : \mathbb{R}^d \rightarrow \mathbb{R}$ with $\phi(v) \neq \phi(w)$ for any two distinct vertices v and w of P' , such that $G_\psi(P)$ is isomorphic to the directed graph $G_{\psi'}(P')$, where

$$\psi'(\{v, w\}) = \begin{cases} (v, w), & \text{if } \phi(v) > \phi(w), \\ (w, v), & \text{otherwise} \end{cases}.$$

In other words, an AOF graph on P is realizable if and only if it is induced by a linear functional on some combinatorially equivalent polytope P' . In particular, if two AOF graphs are isomorphic then either both of them are realizable or none of them can be realized.

2 A Preparatory Classification

An AOF graph $G_\psi(C^3)$ is called *separable* if there are two opposite facets F_1 and F_2 of C^3 such that in $G_\psi(C^3)$ all arcs between F_1 and F_2 have their sink in the same facet. Despite the intuition

that the separable AOF graphs are the ‘nice’ ones, it will turn out that both non-realizable AOF graphs on C^3 are actually separable, one of them even with respect to two pairs of opposite facets.

This section intends to show that (up to isomorphism) all AOF graphs on C^3 are separable, except one. Building on this classification, we will answer the realizability question separately for the separable cases in Subsection 3.1 and Section 4, and for the single non-separable case in Subsection 3.2.

Let us label the vertices of the 3-cube C^3 as shown in Figure 1, and for simplicity identify the AOF graph $G_\psi(C^3)$ with its generating orientation ψ .

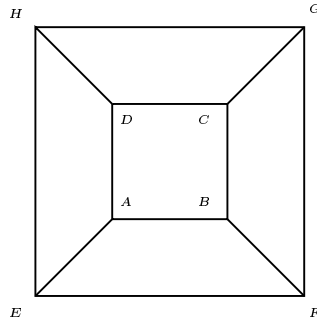


Figure 1: The graph of C^3 with vertices labelled A, \dots, H .

Theorem 1. *Let ψ_0 be the AOF graph depicted in Figure 2. Up to isomorphism, the only non-separable AOF graph on C^3 is ψ_0 .*

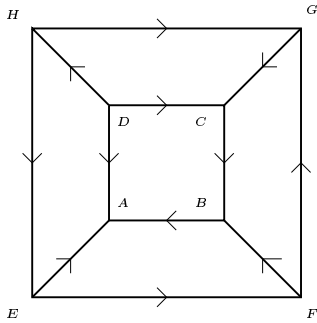


Figure 2: The AOF graph ψ_0 .

Proof. Let ψ be a non-separable AOF graph on C^3 , inducing sink v_{\min} and source v_{\max} . We distinguish three cases:

- (i) v_{\min} and v_{\max} are contained in one edge.
- (ii) v_{\min} and v_{\max} are contained in one facet but not in one edge.
- (iii) v_{\min} and v_{\max} are not contained in one facet.

Let us start with case (i). We can assume $v_{\min} = A$ and $v_{\max} = D$, which implies $H \rightarrow E$ and $C \rightarrow B$. Since ψ is non-separable, we can even conclude $F \rightarrow G$. If $\{E, F\}$ is oriented $E \rightarrow F$, then this enforces $H \rightarrow G$ as well as $F \rightarrow B$, which finally implies $G \rightarrow C$, and thus $\psi = \psi_0$. If $\{E, F\}$ is oriented $F \rightarrow E$, then we must have $G \rightarrow H$, $C \rightarrow G$, and $B \rightarrow F$, i.e., ψ looks as shown in Figure 3. Hence ψ is isomorphic to ψ_0 via exchanging C and H as well as B and E (in

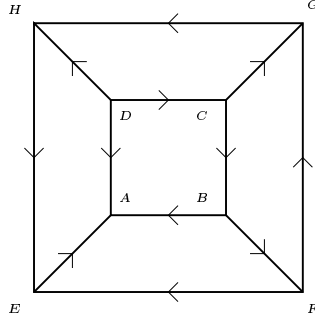


Figure 3: An AOF graph that is isomorphic to ψ_0 .

the standard unit-cube, this corresponds to a reflection at the hyperplane through D, A, G and F).

In case (ii) we can assume $v_{\min} = A$ and $v_{\max} = C$. If $\{F, G\}$ is oriented $G \rightarrow F$, then we must have $E \rightarrow H$ (since ψ is non-separable), which enforces $H \rightarrow D$, therefore $G \rightarrow H$, and thus $F \rightarrow E$, contradicting the fact that ψ is non-separable. Thus, $\{F, G\}$ must be oriented $F \rightarrow G$. This yields $B \rightarrow F$, which then implies $F \rightarrow E$. Since ψ is non-separable we then must have $H \rightarrow G$, but this means that G is a second sink, a contradiction.

Finally, we consider case (iii). We can assume $v_{\min} = A$ and $v_{\max} = G$. Let us first suppose that $\{C, D\}$ is oriented $D \rightarrow C$, implying $C \rightarrow B$ and $H \rightarrow D$. Since ψ is non-separable one deduces both $E \rightarrow H$ and $B \rightarrow F$, and the latter condition enforces $F \rightarrow E$. But now we have an oriented cycle D, C, B, F, E, H, D , which is a contradiction. Thus $\{C, D\}$ must be oriented $C \rightarrow D$. Since ψ is non-separable this implies $E \rightarrow F$, from which $F \rightarrow B$ follows, yielding $D \rightarrow H$ (since ψ is non-separable). From the latter, one deduces $H \rightarrow E$ and from this $B \rightarrow C$ (again, because ψ is non-separable), constituting another oriented cycle C, D, H, E, F, B, C . \square

3 The Realizable Cases

In this section, we prove realizability for all but two of the separable AOF graphs (Subsection 3.1) and the single non-separable one (Subsection 3.2). We do this by explicitly constructing realizations.

3.1 Separable AOF Graphs

We may assume that vertex A is the global sink and that the facet $\{A, B, C, D\}$ is the ‘lower’ facet, meaning that the incident arcs are all incoming. It is easy to see that any such AOF graph is obtained by combining an arbitrary AOF graph for the upper facet with one for the lower facet in which A is the sink. Let us enumerate the possibilities. In the lower facet we can have three situations, see Figure 4.

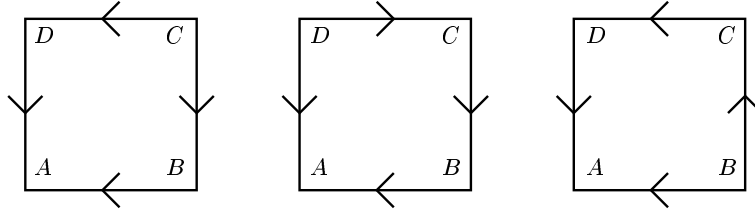


Figure 4: Possible orientations in the lower facet.

Consequently, in the upper facet we must consider twelve situations, depending on where the sink of that facet is.

In the following we present realizations for almost all combinations of these upper and lower facet orientations. All the realizations will have the same ‘vertical walls’ induced by the inequalities

$$4x_2 \geq x_1, \quad 4x_1 \geq x_2, \quad 2x_1 + x_2 \leq 9, \quad x_1 + 2x_2 \leq 9,$$

so that the cube projects onto the plane $x_3 = 0$ in form of the ‘gadget’ shown in Figure 5.

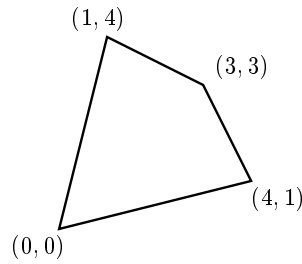


Figure 5: Realization gadget.

Moreover, the objective function will be $\phi(x) = x_3$ in all cases, so vertices are ordered by height. In this setup, we are still free to choose the planes for the top and bottom facet. The possible edge orientations we can (independently) obtain in both facets are exactly the ones induced by linear functionals $\hat{\phi} : \mathbb{R}^2 \mapsto \mathbb{R}$ acting on the projection depicted in Figure 5. For example, the functional $\hat{\phi}(x_1, x_2) = x_1 + x_2$ induces the orientation of Figure 6, and by choosing the plane $x_3 = \hat{\phi}(x_1, x_2) + c$ (c some constant) for one of the facets, we can ‘lift’ this orientation in such a way that it is induced by ϕ .

It is easy to see that the other two orientations of the lower facet as given in Figure 4 are also obtainable in this way, namely with $\hat{\phi}(x_1, x_2) = x_2$ resp. $\hat{\phi}(x_1, x_2) = x_1$ (and the vertices named as in Figure 6).

Let’s consider the upper facet. If the orientation is such that no directed path of length 3 exists (as in the leftmost case of Figure 4), we are done, because all four such orientations are realizable via $\hat{\phi}(x_1, x_2) = \pm x_1 \pm x_2$ and can be combined with the lower facet realizations discussed before. By interchanging the roles of upper and lower facet, we also see that the leftmost case of Figure 4 need not be considered anymore for the lower facet.

In the remaining eight cases for the upper facet, there are two orientations for every possible sink, distinguished by whether the source is the next vertex in clockwise or in counterclockwise

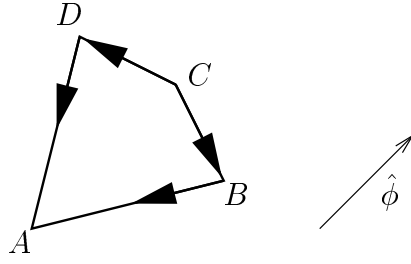


Figure 6: Possible facet orientation.

direction. We can restrict to the cases where the source is the next vertex in clockwise direction, because the other cases are isomorphic to these via interchanging the pairs of vertices B and D as well as F and H .

This means, we are left with one orientation per sink in the upper facet (for a total of four orientations), and the possible combinations with the two remaining orientations of the lower facet are summarized in Figures 7 and 8, where realizations to all but two combinations are given. For the remaining two one indeed does not find a realization using the gadget, for a good reason: they are not realizable at all.

		<p>?</p>	

Figure 7: Realization table for lower facet orientation $D \rightarrow C \rightarrow B \rightarrow A$. The respective linear functionals are always $\hat{\phi}(x_1, x_2) = \pm x_1$ or $\hat{\phi}(x_1, x_2) = \pm x_2$.

3.2 Non-Separable AOF Graphs

Theorem 1 shows that there is (up to isomorphism) only one AOF graph ψ_0 on the 3-cube that is not separable, see Figure 2.

Theorem 2. *The AOF graph ψ_0 is realizable.*

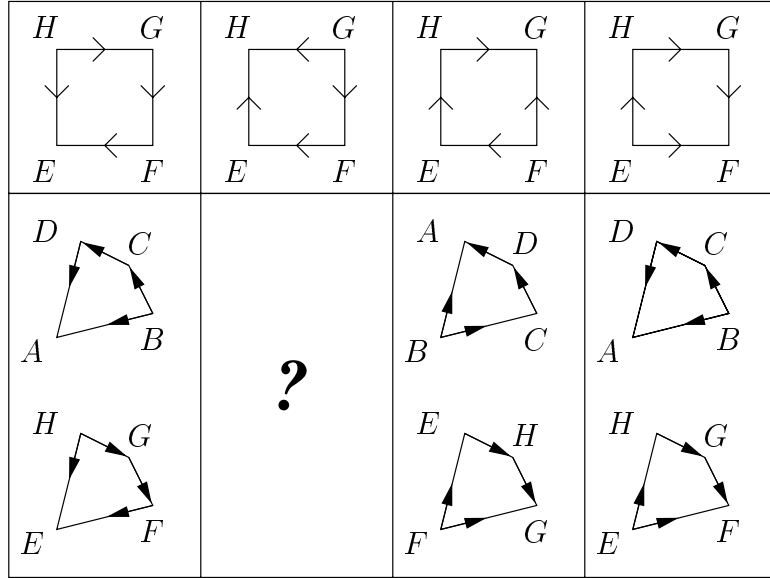


Figure 8: Realization table for lower facet orientation $B \rightarrow C \rightarrow D \rightarrow A$. Again, the respective linear functionals are always $\hat{\phi}(x_1, x_2) = \pm x_1$ or $\hat{\phi}(x_1, x_2) = \pm x_2$.

Proof. To find a realization of the AOF graph ψ_0 , we slightly modify the gadget of Subsection 3.1 to the two-dimensional polytope P_0 that is shown in Figure 9. Consider the (combinatorial) 3-

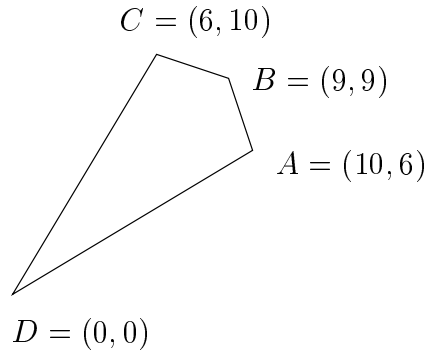


Figure 9: The modified gadget P_0 .

cube $P_0 \times [0, 2.5]$, where we label the vertices of the lower facet as shown in Figure 9, and the ones in the upper facet (as in the previous sections) by letting E be above A , F above B , G above C , and H above D . It suffices to rotate some of the defining halfspaces (such that the polytope stays a combinatorial 3-cube) suitably until the order of the vertices with respect to their x_1 -coordinates is D, H, E, F, G, C, B, A . The linear functional that induces ψ_0 then is $\phi(x_1, x_2, x_3) = -x_1$.

This procedure was extremely simplified by the software tool `polymake` (written by Evgenij Gawrilow and Michael Joswig [7]) that enabled us to find the correct rotations by “try and error”. We start by rotating (all upcoming rotations will be directed towards the interior of the current polytope) the facet $\{A, B, F, E\}$ around $\{A, B\}$, as well as $\{B, C, G, F\}$ around $\{B, C\}$.

Then the upper facet becomes smaller, and the “top view” of the resulting polytope is shown in Figure 10 (a). Next, we have to push G and F to the right of E , which can be achieved by rotating the facet $\{E, F, G, H\}$ around $\{E, H\}$. Figure 10 (b) shows that we are basically done now. The only thing that remains to be done is to bring H , which is still above D , to the right of D . Rotating the facet $\{D, H, G, C\}$ around $\{D, C\}$ yields this (see Figure 10 (c)).

We finally give the exact coordinates of the realization. After the rotations the facets of the polytope are described by the following inequalities:

$$\begin{array}{rcllcl}
 \{D, H, G, C\} : & -500x_1 & +300x_2 & +250x_3 & \leq & 0 \\
 \{A, E, H, D\} : & 300x_1 & -500x_2 & & \leq & 0 \\
 \{A, B, F, E\} : & 300x_1 & +100x_2 & +1000x_3 & \leq & 3600 \\
 \{B, C, G, F\} : & 100x_1 & +300x_2 & +1000x_3 & \leq & 3600 \\
 \{A, B, C, D\} : & & & -x_3 & \leq & 0 \\
 \{E, F, G, H\} : & -21x_1 & +35x_2 & +100x_3 & \leq & 250
 \end{array}$$

The rotations of $\{A, B, F, E\}$ and $\{B, C, G, F\}$ were obtained by adding a multiple of 1000 times the equation $x_3 = 0$ (describing the lower facet $\{A, B, C, D\}$) to the respective defining inequality. Similarly, rotating facet $\{D, H, G, C\}$ was done (here, we used a multiple of 250). The rotation of the upper facet $\{E, F, G, H\}$ was achieved by adding the $(-\frac{7}{100})$ -fold multiple of the equation $300x_1 - 500x_2 = 0$ that defines $\{A, E, H, D\}$ to the inequality defining $\{E, F, G, H\}$.

The vertices of the resulting polytope are: $A = (10, 6, 0)$, $B = (9, 9, 0)$, $C = (6, 10, 0)$, $D = (0, 0, 0)$, $E = (55/18, 11/6, 5/2)$, $F = (55/13, 55/13, 125/64)$, $G = (135/29, 199/29, 156/145)$, and $H = (125/64, 75/64, 5/2)$. \square

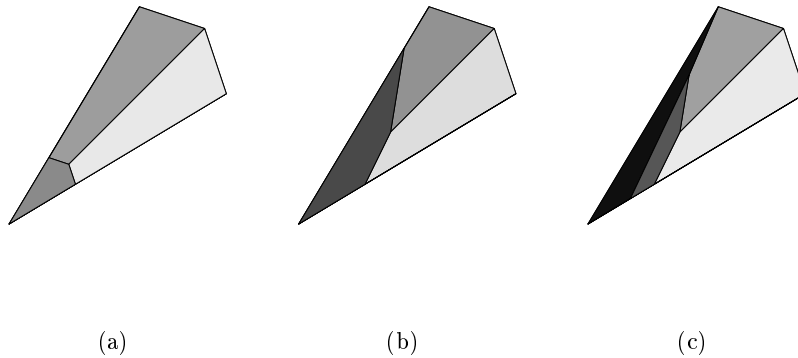


Figure 10: Constructing a cube on which ψ_0 can be realized

4 The Non-Realizable Cases

In the preceding sections we have shown the realizability of all AOF graphs on C^3 except for ψ_1 and ψ_2 (see Figure 11). These two AOF graphs are the ones corresponding to the question marks in Figures 7 and 8.

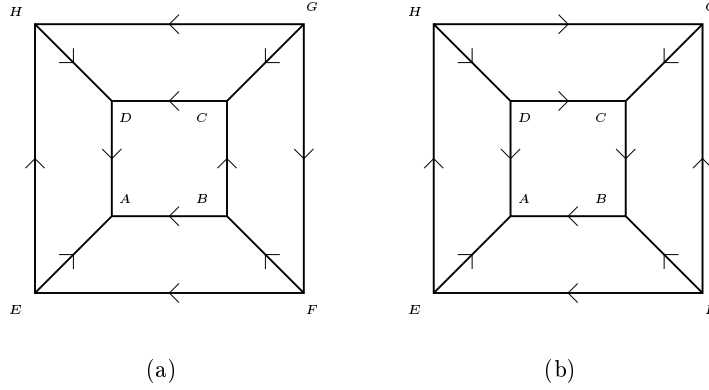


Figure 11: The AOF graphs ψ_1 (a) and ψ_2 (b).

Theorem 3. *The AOF graphs ψ_1 and ψ_2 are not realizable.*

Proof. Suppose we have a realization of ψ_1 by some combinatorial 3-cube that is the intersection of the halfspaces $\mathcal{H}_1^+, \dots, \mathcal{H}_6^+$ and by some linear function $\phi_1 : \mathbb{R}^3 \rightarrow \mathbb{R}$.

Let \mathcal{H}_6^+ be the halfspace that defines the facet $\{D, C, G, H\}$. Consider the polytope $P := \mathcal{H}_1^+ \cap \dots \cap \mathcal{H}_5^+$. Suppose that P has more vertices than $A, B, F,$ and E . Then the graph of P arises from the graph of our 3-cube either by contraction of the whole facet $\{D, C, G, H\}$, or by contraction of $\{H, D\}$ and $\{G, C\}$, or by contraction of $\{H, G\}$ and $\{D, C\}$. (To see this note that P has at most six vertices by the Upper Bound Theorem (see e.g. [14]), four of which (namely A, B, F, E) are of degree exactly three and form a quadrangle in the Schlegel diagram of P based at $\{A, B, F, E\}$. Since the remaining at most two vertices have degree at least three, it easily follows that this Schlegel diagram of P is one of the three graphs in Figure 12, corresponding to the three different kinds of contractions). In the AOF graph induced by ϕ_1

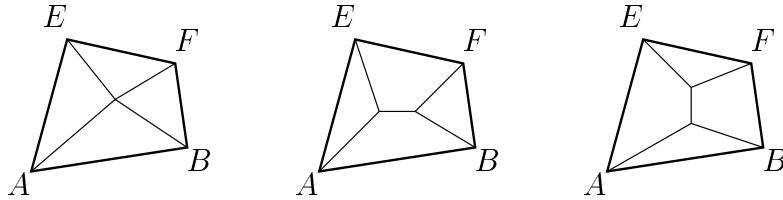


Figure 12: Possible Schlegel diagrams of P based at $\{A, B, F, E\}$.

on P ,¹ the orientations of the edges that are incident to A, B, F or E stay the same as in ψ_1 . But then there are two adjacent edges $\{G, C\}$ and $\{G, H\}$ in the facet $\{D, C, G, H\}$ defined by \mathcal{H}_6 whose contraction each gives a directed cycle (with respect to ψ_1). Thus each of the three cases leads to a contradiction, and hence, $A, B, F,$ and E must be the only vertices of P .

Let the halfspace \mathcal{H}_1^+ define the facet $\{A, B, F, E\}$ which is opposite to $\{D, C, G, H\}$. Since the contractions of the two adjacent edges $\{A, B\}$ and $\{A, E\}$ of the facet $\{A, E, F, B\}$ each

¹Note that in case of two “new” vertices V and W we can always achieve that ϕ_1 assigns different values to V and W by slightly perturbing ϕ_1 , so that the edge $\{V, W\}$ actually has an orientation with respect to ϕ_1 .

give directed cycles (with respect to ψ_1) as well, it follows that analogously the polytope $P' := \mathcal{H}_2^+ \cap \dots \cap \mathcal{H}_6^+$ has no more vertices than D , C , G , and H .

But then, the polytope $\mathcal{H}_2^+ \cap \dots \cap \mathcal{H}_5^+$ has no vertices at all, and hence the edges $\{H, E\}$, $\{D, A\}$, $\{C, B\}$, and $\{G, F\}$ are pairwise parallel (otherwise two of their supporting lines would intersect and define a vertex), which is impossible, since this would imply that the objective function ϕ_1 induces the same orientation on all of them. Thus, ψ_1 cannot be realizable.

The proof for ψ_2 is similar. P and P' are now defined with respect to the opposite facets $\{A, D, H, E\}$ and $\{B, C, G, F\}$, with P (resp. P') being the intersection of the halfspaces corresponding to the facets different from $\{A, D, H, E\}$ (resp. $\{B, C, G, F\}$). Again, we want to show that P and P' have no more than the obvious four vertices each, from which we get a contradiction as before. So, assume that P has additional vertices, in which case its graph arises from the cube graph by contracting $\{A, D\}$ and $\{E, H\}$, or $\{A, E\}$ and $\{D, H\}$, or both. If $\{A, D\}$ gets contracted, then we obtain a directed cycle (recall that edges incident to B, C, G or F keep their orientations). Otherwise, $\{A, E\}$ and $\{D, H\}$ get contracted. If the new edge $\{D/H, A/E\}$ is oriented $A/E \rightarrow D/H$ then we have a directed cycle again, and if it is oriented $D/H \rightarrow A/E$, we obtain a second global source D/H , which cannot happen if the orientation comes from a linear objective function ϕ_2 . It follows that P cannot have more vertices.² The corresponding statement for P' is derived analogously, using the fact that the contraction of $\{G, F\}$ yields a directed cycle, while contracting $\{C, G\}$ and $\{B, F\}$ either gives a directed cycle (if the new edge $\{C/G, B/F\}$ is oriented $C/G \rightarrow B/F$) or a second global sink C/G (if $\{C/G, B/F\}$ is oriented $B/F \rightarrow C/G$). \square

References

- [1] I. Adler. *Abstract Polytopes*. PhD thesis, Dept. Operations Research, Stanford University, 1971.
- [2] R. G. Bland. New finite pivoting rules for the simplex method. *Math. Operations Research*, 2:103–107, 1977.
- [3] V. Chvátal. *Linear Programming*. W. H. Freeman, New York, NY, 1983.
- [4] B. Gärtner. A subexponential algorithm for abstract optimization problems. *SIAM J. Comput.*, 24:1018–1035, 1995.
- [5] B. Gärtner. Geometry vs. combinatorics in linear programming. Manuscript, 1998.
- [6] B. Gärtner, M. Henk, and G. M. Ziegler. Randomized simplex algorithms on Klee-Minty cubes. Manuscript (submitted), 1996.
- [7] E. Gawrilow and M. Joswig. polymake. <http://www.math.TU-Berlin.de/diskregeom/polymake/doc/>, 1997/98.
- [8] G. Kalai. A subexponential randomized simplex algorithm. In *Proceedings of the 24th Annual ACM Symposium on the Theory of Computing*, pages 475–482, Victoria, 1992. ACM Press.
- [9] G. Kalai. Linear programming, the simplex algorithm and simple polytopes. *Math. Programming*, 79:217–233, 1997.

²As for ϕ_1 , it may be necessary to perturb ϕ_2 slightly.

- [10] J. Matoušek, M. Sharir, and E. Welzl. A subexponential bound for linear programming. *Algorithmica*, 16:498–516, 1996.
- [11] J. Matoušek. Lower bounds for a subexponential optimization algorithm. *Random Structures & Algorithms*, 5(4):591–607, 1994.
- [12] K. Williamson Hoke. Completely unimodal numberings of a simple polytope. *Discrete and Applied Math.*, 20:69–81, 1988.
- [13] N. Zadeh. What is the worst case behavior of the simplex algorithm? Technical Report 27, Dept. Operations Research, Stanford University, 1980.
- [14] G. M. Ziegler. *Lectures on Polytopes*, volume 152 of *Graduate Texts in Mathematics*. Springer-Verlag, 1994.